Contrasting Relationship between Tropical Western North Pacific Convection and Rainfall over East Asia during Indian Ocean Warm and Cold Summers

JIE SONG AND CHONGYIN LI

LASG, Institute of Atmospheric Physics, Chinese Academy of Sciences, Beijing, China

(Manuscript received 1 April 2013, in final form 6 November 2013)

ABSTRACT

Using daily data, this study compares the subseasonal seesaw relationship between anomalous tropical western North Pacific (WNP) convection and anomalous rainfall over subtropical East Asia during boreal summers (June–August) in which the Indian Ocean (IO) sea surface temperature is either warmer or colder than normal. It is found that the precipitation anomalies over central-eastern China (25°–35°N, 110°–120°E) associated with the anomalous tropical WNP convection activities during the IO cold summers are weaker and less evident compared to that in the IO warm summers, indicating the seesaw relationship in the IO cold summers becomes obscure. This contrasting seesaw relationship between the IO warm and cold summers is attributed to different patterns of anomalous moisture transportation and vertical motion over central-eastern China. The anomalous circulations associated with the anomalous tropical WNP convection [the Pacific–Japan (PJ) pattern] during the IO warm and cold summers show that, relative to the IO warm summers, the Japan action center of the PJ pattern has an evident northwestward displacement in the IO cold summers. It is argued that this northwestward displacement of the Japan action center plays a key role in the formation of the distinct seesaw relationship through modifying the anomalous moisture transportation and vertical motion.

1. Introduction

A remote out-of-phase linkage between anomalous convective activities over the tropical western North Pacific (WNP; 10°–25°N, 100°–140°E) and rainfall anomalies over subtropical East Asia (25°–35°N, 110°–150°E) in boreal summer [June–August (JJA)] on both interannual and subseasonal time scales has been revealed in previous studies (e.g., Nitta 1987; Huang and Sun 1992). Suppressed (enhanced) convective activities over the tropical WNP tend to strengthen (weaken) summer rainfall over subtropical East Asia (from the Yangtze River valley to southern Japan) through a meridional teleconnection: the Pacific–Japan (PJ; Nitta 1987) or East Asia–Pacific (EAP; Huang and Sun 1992) pattern. We refer to the remote out-of-phase linkage between tropical WNP convection and summer rainfall over subtropical East Asia as the ''seesaw relationship.''

The PJ pattern, characterized by a zonally elongated meridional dipole of anomalies, emanates from the tropical WNP and extends to extratropical East Asia along the East Asian coast. In the lower troposphere, below (above)-normal convective activities over the tropical WNP are associated with a zonally elongated anomalous anticyclone (cyclone) around the center of the anomalous convection and a zonally elongated anomalous cyclone (anticyclone) over the midlatitudes of East Asia around southern Japan. Correspondingly, the WNP subtropical high (WNPSH) extends westward (retreats eastward) and displaces equatorward (poleward) when the intensity of the tropical WNP convective activities is weaker (stronger) (e.g., Lu 2001). This leads to a stronger (weaker) moisture transportation into subtropical East Asia by the southwesterly flow along the western rim of the WNPSH and consequently strengthened (weakened) precipitation over this region. Kosaka and Nakamura (2010) also indicated that, under the summer monsoon background flow in East Asia, anomalous reverse vertical motion tends to be dynamically forced around the tropical WNP and subtropical East Asia by the PJ-like meridional dipole pattern, which is also helpful in constructing and reinforcing the seesaw relationship. We refer to the two nodes of the PJ

Denotes Open Access content.

Corresponding author address: Jie Song, LASG, 40 Hua Yan Li, Chao Yang District, P.O. Box 9804, Beijing 100029, China.
E-mail: song_jie@mail.iap.ac.cn

DOI: 10.1175/JCLI-D-13-00207.1

dipolar pattern as the WNP action center and the Japan action center, respectively.

The PJ pattern is considered a meridionally propagating Rossby wave train triggered by anomalous tropical WNP convection (e.g., Kurihara and Tsuyuki 1987). Kosaka and Nakamura (2006, 2010) documented and examined the three-dimensional structure and dynamic mechanism of the PJ pattern. Their studies suggested that the PJ pattern could be regarded as an internal dynamic mode of the atmosphere embedded in the summer monsoon background circulation in East Asia, which can be most efficiently excited by tropical WNP convection. In addition, Lu and Lin (2009) indicated that the subtropical precipitation anomalies associated with the PJ pattern also play a role in forming and maintaining this pattern.

This seesaw relationship between WNP convection and East Asian summer rainfall anomalies is important in understanding the variations of the East Asia summer monsoon (EASM). Actually, it is the dominant mode in the variability of the EASM on both interannual and subseasonal time scales (e.g., Wang et al. 2008; Wu et al. 2009; and many others). In addition, a number of summer monsoon indices defined by different methods also depict or reflect this kind of seesaw relationship (e.g., Wang and Lau 2001; Li and Zeng 2002; Huang 2004; Lee et al. 2005; Wang et al. 2008). Even the El Niño–Southern Oscillation (ENSO; Trenberth et al. 1998), the most important interannual signal of the tropical atmosphere, impacts the EASM largely through anomalous WNP convection and a PJ-like pattern (e.g., Wu and Wang 2002). In addition to ENSO, sea surface temperature (SST) anomalies in the Indian Ocean (IO), which are another important interannual signal of the tropical atmosphere, also impact variations of the EASM by modulating the tropical WNP convection and a PJ-like pattern via anomalous surface wind stresses associated with the Kelvin wave (e.g., Xie et al. 2009). Therefore, the importance of the seesaw relationship is paramount. Some previous studies have also suggested that there is a similar reverse relationship between the EASM/northeast Asian summer monsoon (NEASM; e.g., Lee et al. 2005) and the western North Pacific summer monsoon (WNPSM; Wang and Lau 2001). In our understanding, this reverse relationship between the EASM/NEASM and the WNPSM is equivalent to the seesaw relationship we discuss here, since the EASM/NEASM index is highly correlated with variations in rainfall over subtropical East Asia and the WNPSM index is highly correlated with anomalies in tropical WNP convection.

The seesaw relationship and the associated teleconnection pattern are robust. However, they are not always stable, particularly on decadal time scales. Wu and Wang (2002) found that the influences of anomalous WNP convection on summer rainfall in East Asia and the associated teleconnection patterns were noticeably different before and after the late 1970s. Kwon et al. (2005) found that the reverse relationship between the WNPSM and the EASM was much stronger from 1994 to 2004 than it was before 1994 (1979–93), suggesting that the seesaw relationship changes on decadal time scales. Yim et al. (2008) confirmed the low-frequency change in the relationship between the EASM and WNPSM in a long-term integration of model results, concluding that the changing relationship between the EASM and the WNPSM is a result of the interference of ENSO-related rainfall variability over East Asia. Lin et al. (2009) examined the changes in the PJ-like meridional teleconnection in terms of the variability of the East Asian jet in the upper troposphere and found that in June this teleconnection was less evident after the late 1970s. They suspected that the weakening of background vertical easterly shear over the tropical WNP after the late 1970s was responsible for this change.

A comprehensive understanding of the changes in the seesaw relationship and PJ pattern are important to understand and predict the variability of EASM. However, all the foregoing studies focused on the change in the seesaw relationship and PJ pattern on decadal time scales. In this study, using daily data, we deliver a new finding about the change in the seesaw relationship but on the more fundamental subseasonal time scales. We find that the subseasonal remote out-of-phase linkage between tropical WNP convection and summer rainfall over subtropical East Asia is considerably different between summers that the overall SST fields of the IO are warmer and colder than normal. Our emphasis is on understanding the physical processes beneath the change in the seesaw relationship. The rest of this paper is organized as follows: Section 2 describes the datasets and analysis methods used in this study. In section 3, we demonstrate and discuss the contrast of the seesaw relationship. The details of plausible physical mechanisms responsible for this contrast are investigated and discussed in sections 4 and 5. In the last section, we present a summary and further discussion.

2. Data and methods

a. Data

The reanalysis data used in this study are the National Centers for Environmental Prediction–National Center for Atmospheric Research (NCEP–NCAR) Reanalysis-1 daily data (Kalnay et al. 1996). We also use the National Oceanic and Atmospheric Administration (NOAA)

interpolated outgoing longwave radiation (OLR) daily data to represent variations in the tropical convection. The horizontal resolution of the NCEP–NCAR and the OLR data is 2.5° × 2.5°. In addition, NOAA extended reconstructed SST, version 3b (ERSST v3b) data are also used in this study. The horizontal resolution of the SST data is 2.0° × 2.0°. To well depict the change in the seesaw relationship on subseasonal time scales, high-quality daily precipitation data are required. In this study, we use the Asian Precipitation—Highly Resolved Observational Data Integration towards Evaluation of Water Resources (APHRODITE) daily precipitation data (Yatagai et al. 2012). The APHRODITE data, created primarily with data obtained from a rain gauge observation network, are state-of-the-art daily precipitation data with a high-resolution grid (0.25° × 0.25°) for Asian land area. The daily OLR data cover the time period from 1 June 1974 to the present. The APHRODITE daily precipitation data (v0902) cover the time period from 1 January 1961 to 31 December 2004. Unfortunately, the OLR data are missing from 17 March 1978 to 31 December 1978. Therefore, we restrict the time period of our study to the 26 boreal summers (JJA) from 1979 to 2004, which yield 2392 days of data.

b. Analysis methods

To depict variations in convective activities over the tropical WNP, a daily WNP convection index is defined as the area mean daily OLR over the maximum variance region of the OLR (10°–25°N, 100°–140°E). We then normalize the time series of the daily WNP convection index. A positive (negative) WNP convection index denotes a suppression (enhancement) of tropical WNP convective activities, since the OLR and tropical convective activities are anticorrelated. We also define a seasonal mean IO SST index by averaging the SST in JJA over the IO Basin (20°S–20°N, 40°–100°E) to represent the interannual variability of the summer mean SST of the IO. Before the area averaging, the daily OLR and monthly SST data were weighted by the square root of the cosine of latitude to account for the decrease in grid area toward the pole.

Using the time series of the seasonal mean IO SST index, the 5 warmest and 5 coldest summers of the IO were selected from the 26 summers. The five warmest summers of the IO (IO warm summers) are 1983, 1987, 1998, 2002, and 2003, and the five coldest summers of the IO (IO cold summers) are 1984, 1985, 1986, 1989, and 1994. Composite anomalous SST fields for the IO warm and cold summers show that the overall patterns of the IO SST anomalies are indeed significantly warmer and colder than normal (not shown). It should be pointed out that the OLR variance maps and the standard deviations of the WNP convection index of the IO warm and cold summers do not have evident differences (not shown). In this study, the term "anomalies" is defined as the deviation from the seasonal cycle, which is defined as the long-term mean of each calendar day in these 26 summers. To avoid a possible contamination from the interannual variability on the comparison of the subseasonal seesaw relationship between the IO warm and cold summers, the interannual variability is removed from the daily anomalies by subtracting the summer mean of the daily anomalies of each year. In this study, we primarily use linear regression analysis. All the regressed results in this study correspond to one standard deviation of the tropical WNP convection index. We discuss only the results for the positive tropical WNP convection index, since the regression is linear. In this study, the statistical significance of regression result is established by using the Student's t statistic,

$$t = r\sqrt{N_{\mathrm{dof}} - 2}\Big/\sqrt{1 - r^2},$$

where r denotes the correlation coefficient. The effective number of degrees of freedom N_{dof} is evaluated by using

$$N_{\mathrm{dof}} = N(1 - r_1 r_2)/(1 + r_1 r_2),$$

where N is the sample size and r_1 and r_2 are the lag-1 autocorrelations for the two time series considered (Bretherton et al. 1999). The formula for the linear regression is $y = bx + a$. Then we evaluate the significance of difference of the regression results between the IO cold and warm summers by using the Student's t statistic,

$$t = (b_1 - b_2)/\sqrt{\mathrm{MS}_e(1/S_{x1} + 1/S_{x2})}, \quad \text{where}$$

$$\mathrm{MS}_e = [(N_1 - 2)\mathrm{MS}_1 + (N_2 - 2)\mathrm{MS}_2]/(N_1 + N_2 - 4),$$

$$\mathrm{MS}_i = (S_{yi} - S_{xi,yi}/S_{xi})/(N_i - 2),$$

$$S_{yi} = \sum(y_i - \overline{y_i})^2, \quad \text{and}$$

$$S_{xi,yi} = \sum(x_i - \overline{x_i})(y_i - \overline{y_i}),$$

for $i = 1$ and 2, and b_1 and b_2 are the regression coefficient b for the IO cold and warm summers; and N_1 and N_2 are the sample size of the IO cold and warm summers. The overbar denotes time mean.

3. Contrast in the seesaw relationship between the IO warm and cold summers

In this section, the contrast of the seesaw relationship during the IO warm and cold summers is presented and

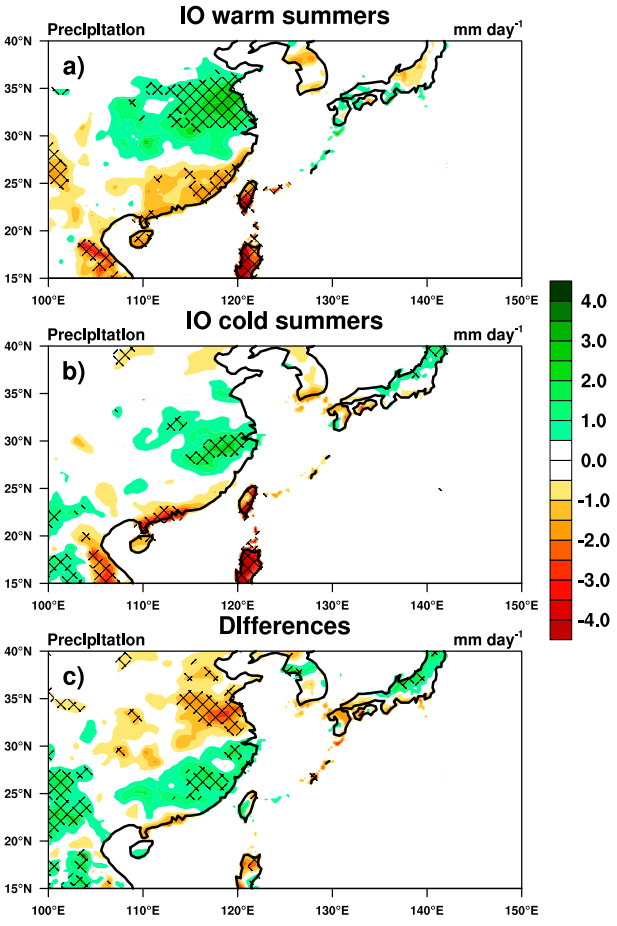

FIG. 1. Anomalous daily precipitation (mm day^{-1}) regressed onto the daily tropical WNP convection index in JJA during the IO (a) warm and (b) cold summers and (c) their differences (IO cold summers minus IO warm summers). Hatched regions denote the regressed precipitation anomalies or the differences at the 95% confidence level.

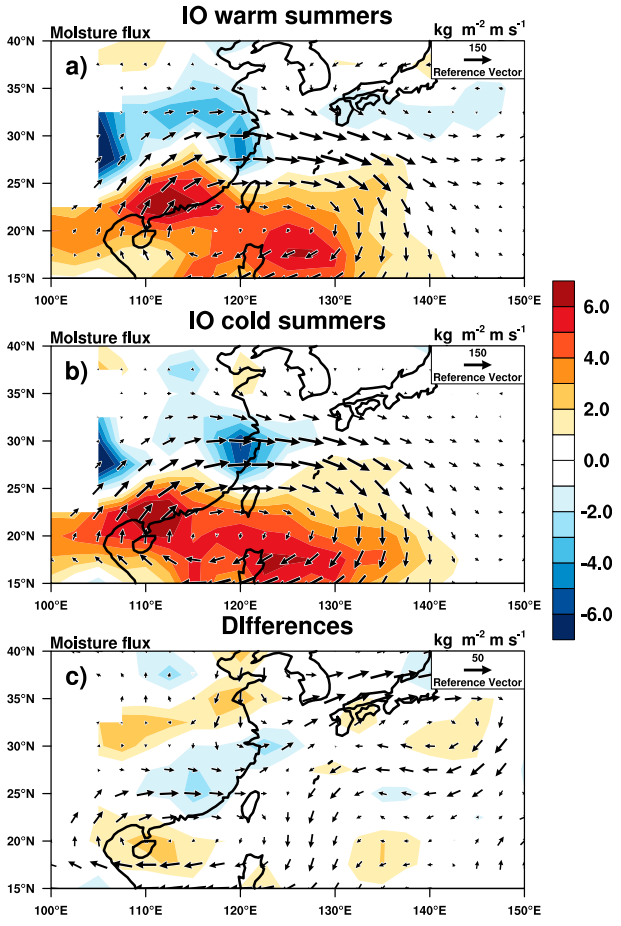

FIG. 2. As in Fig. 1, but for anomalous daily moisture flux integrated from 1000 to 300 hPa (vectors). Shaded areas denote the corresponding horizontal divergence of the regressed moisture flux (10^{-5} kg m^{-2} s^{-1}).

discussed. To demonstrate the contrast of the seesaw relationship, anomalous daily precipitation regressed against the tropical WNP convection daily index during the IO warm and cold summers, as well as their differences (IO cold summers regressed results minus IO warm summers regressed results), is shown in Fig. 1. Generally speaking, the out-of-phase relationship of the precipitation anomalies between subtropical East Asia and the tropical WNP is observed in both the IO warm and cold summers. However, the domain of the positive anomalies over central-eastern China (25°–35°N, 110°–120°E) during the IO cold summers is smaller compared to that in the IO warm summers, indicating that the seesaw relationship becomes less evident in the IO cold summers (see Figs. 1a,b). In addition, we also notice that the overall anomalous rainfall pattern in the IO warm summers has a slight northward displacement. The center of the positive rainfall anomalies over central-eastern China shifts roughly 5° northward (from 28° to 33°N) in the IO warm summers compared to the IO cold summers. Besides that, significant negative anomalies are observed in southeast China in the IO warm summers (see Fig. 1a; 20°–25°N, 110°–120°E). However, they can be detected only in the marginal regions along the coastline of southeast China in the IO cold summers (see Fig. 1b). This northward displacement of the precipitation anomalies between the IO warm and cold summers is also perceived from the differences shown in Fig. 1c.

Moisture supply and atmospheric vertical motion are two factors that are crucial to precipitation. Figure 2 shows corresponding anomalous moisture transportation integrated from 1000 to 300 hPa over East Asia for the IO warm and cold summers, as well as their differences (IO cold summers minus IO warm summers). Consistent with the evident positive rainfall anomalies shown in Fig. 1a,

there are greater anomalous moisture fluxes converging over central-eastern China during the IO warm summers (Fig. 2a). In contrast, the converging regions of the anomalous moisture flux shrink obviously and can be found only in the lower reaches of the Yangtze River valley during the IO cold summers (Fig. 2b). These discrepancies are highlighted in their differences (Fig. 2c). Compared to the IO warm summers, there are south-directed moisture fluxes resulting divergence of the anomalous moisture flux during the IO cold summers over the north part of central-eastern China, which is clearly a disadvantage of the emergence of the anomalous precipitation over there. In addition, anticyclone-like moisture flux anomalies are found southeast of Japan. We believe that this is related to the northwestward shift of the Japan action center of the PJ pattern during the IO cold summers (which will be discussed in section 4).

The anomalous daily isobaric-coordinate vertical velocity ω regressed against the daily tropical WNP convection index for the IO warm and cold summers and their differences (IO cold summers minus IO warm summers) are presented in Fig. 3. Regions with an anomalous ascending (descending) motion are in good correspondence with regions of positive (negative) precipitation anomalies in either the IO warm or cold summers. However, the regressed vertical motion patterns for the IO warm and cold summers are distinctly different. In the IO cold summers, the evident anomalous ascending motion over central-eastern China is weaker, which is consistent with the weaker precipitation anomalies over this region that we observed in Fig. 1b. Besides that, an area with significant anomalous descending motion is found around the Yellow Sea and Bohai Sea regions (34°–40°N, 115°–125°E). This is consistent with the weak negative precipitation anomalies over that region (see Fig. 1b). From the differences shown in Fig. 3c, there is a stronger descending motion over central-eastern China in the IO cold summers, which certainly goes against the positive precipitation anomalies over there.

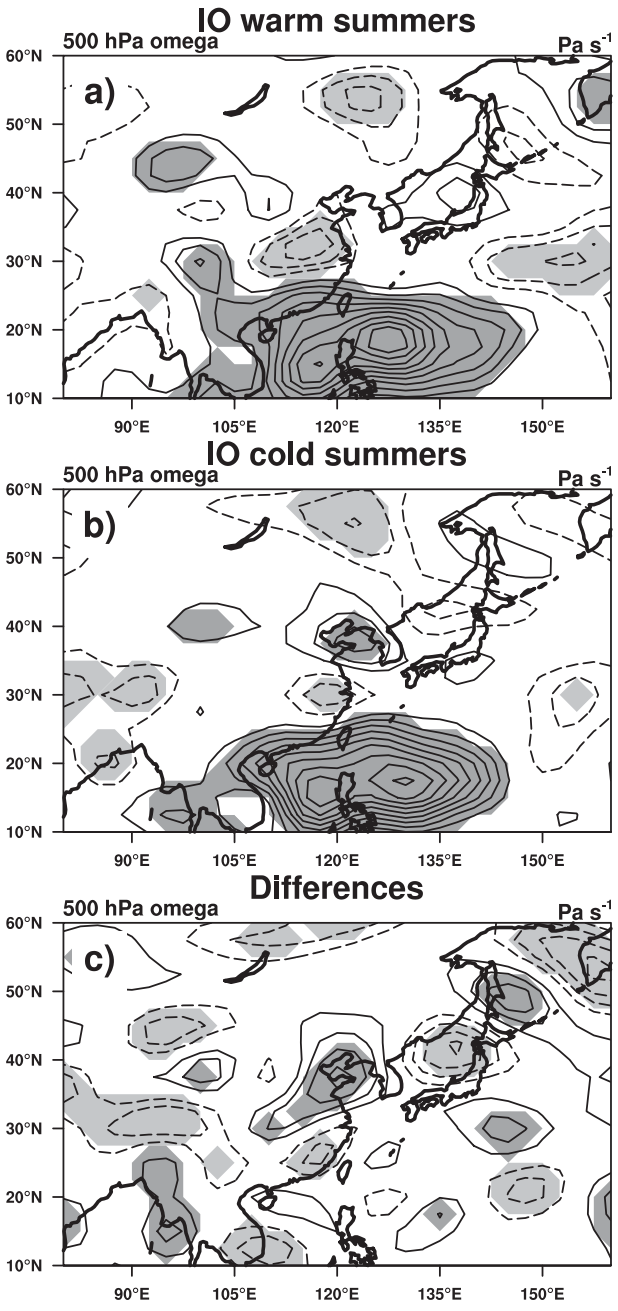

FIG. 3. As in Fig. 1, but for anomalous daily ω at 500 hPa. Solid (dashed) contours represent positive (negative) values, denoting vertical descending (ascending) motion. The zero contours are omitted. The regressed results and their differences at the 95% confidence level are shaded. The contour interval is 4×10^{-3} Pa s^{-1}.

4. Interpretation

The regressed results during the IO warm and cold summers presented in section 3 reveal that the out-of-phase relationship between tropical WNP convection and precipitation over subtropical East Asia is less evident in the IO cold summers, which can be directly attributed to changes in the anomalous moisture transportation (see Fig. 2) and the anomalous vertical motion (see Fig. 3). However, the fundamental physical processes responsible for the contrast of seesaw relationship, especially for the weakened precipitation anomalies over central-eastern China during the IO cold summers, are still unclear. In this section, we find that, relative to the IO warm summers, the Japan action center of the PJ pattern during the IO cold summers has an evident northwestward displacement, which plays a key role in determining the contrast of the seesaw relationship. This

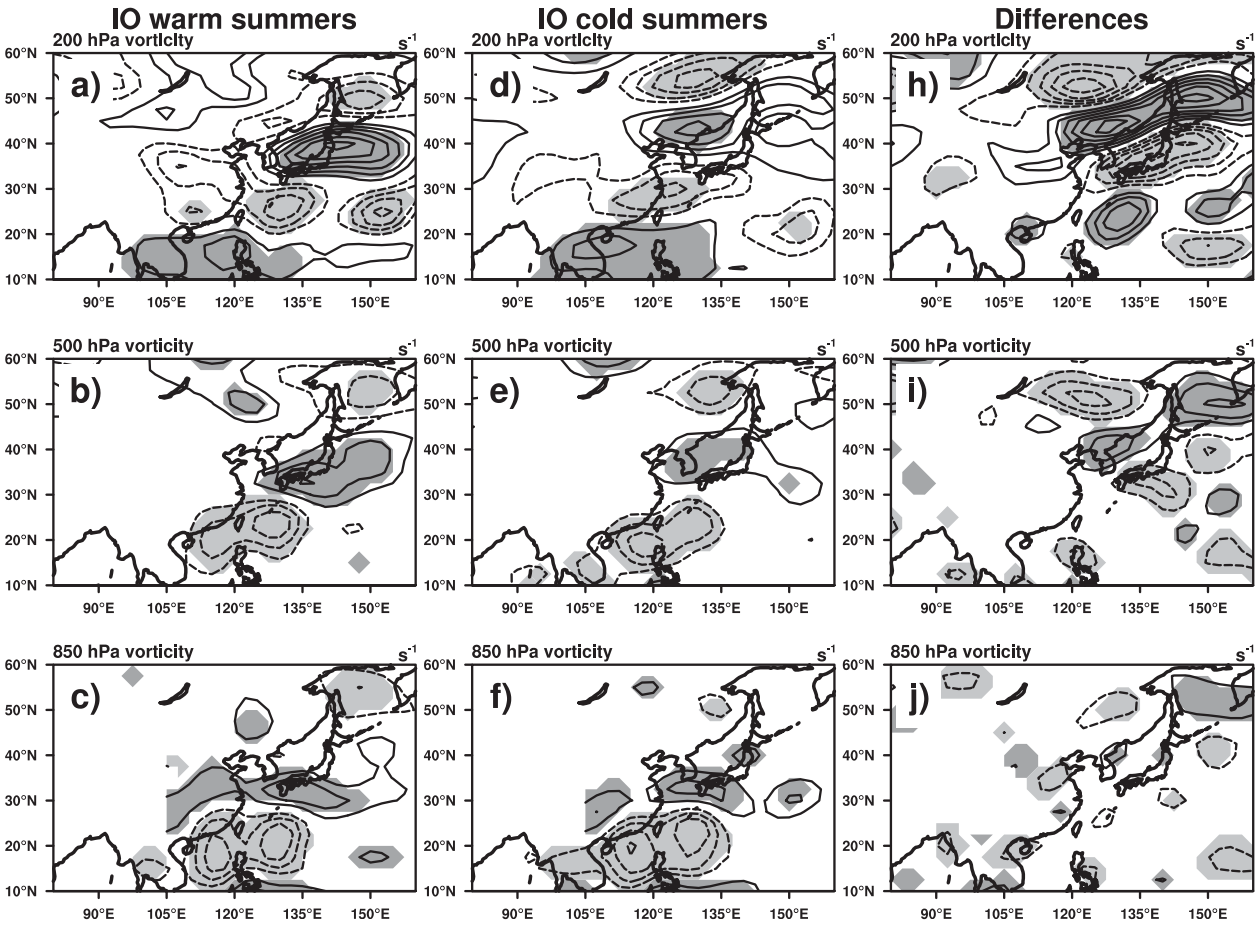

FIG. 4. As in Fig. 1, but for the anomalous daily vorticity at (bottom) 850, (middle) 500, and (top) 200 hPa. (a)–(c) The IO warm summers, (d)–(f) the IO cold summers, and (h)–(j) their differences (IO cold summers minus IO warm summers). Solid (dashed) contours represent positive (negative) values and the zero contours are omitted. The regressed results and their differences at the 95% confidence level are shaded. The contour interval is $2 \times 10^{-6}\,s^{-1}$.

northwestward displacement of the Japan action center not only induces northerlies over central-eastern China, thus reducing the northeast-directed moisture fluxes, but also, under the summer monsoon background circulation of East Asia, dynamically forces anomalous descending motion around the Yellow Sea and Bohai Sea regions, counteracting the anomalous ascending motion over central-eastern China. The combined effect of the two processes suppresses the precipitation anomalies associated with the tropical WNP convection over central-eastern China during the IO cold summers.

a. Different PJ patterns

To demonstrate the northwestward displacement of the Japan action center during the IO cold summers, Fig. 4 shows the daily vorticity anomalies regressed against the daily tropical WNP convection index at the 200-, 500-, and 850-hPa levels for the IO warm and cold summers. The most distinct characteristic of the PJ pattern is a meridional dipole of anomalous vorticity with an apparent poleward tilt with height, which can be observed in the IO warm and cold summers from the lower to upper troposphere. This is consistent with the results of Kosaka and Nakamura (2010, see their Fig. 2). However, there is a notable bias of the anomalous vorticity patterns between the IO warm and cold summers: relative to its position in the IO warm summers, the Japan action center has a northwestward displacement. This northwestward shifting can be observed from the lower to upper troposphere but is more pronounced in the upper troposphere (see Figs. 4a,d). Besides that, in the lower troposphere, the positive vorticity anomalies over central-eastern China during the IO cold summers are slightly weaker compared to those in the IO warm summers (see Figs. 4c,f), which might be related to the weaker positive precipitation anomalies over there.

b. Moisture transportation

We argue that the anomalous southward-directed moisture fluxes over the north part of central-eastern China between the IO cold and warm summers shown in Fig. 2c can be, at least partly, explained by the northwestward displacement of the Japan action center. Under the effect of cyclonic anomalies, there are northerly anomalies appearing at the west sides of the Japan action center. Therefore, the northwestward shifting of the Japan action center during the IO cold summers would tend to arouse anomalous northerlies over the north part of central-eastern China, which offset the anomalous northeastward moisture transportation resulting from the southwesterly associated with the WNP anticyclone. Besides that, the anticyclone-like moisture flux anomalies over southeast of Japan shown in Fig. 2c are also related to the northwestward displacement of the Japan action center, since the northwestward displacement would also produce anticyclonic anomalies at the east sides of the Japan action center (see Fig. 4h).

c. Vertical motion

One might argue that the weak anomalous ascending motion over central-eastern China shown in Fig. 3b is related to the weaker positive precipitation anomalies over there. In this subsection, we provide some pieces of evidence to prove that the northwestward displacement of the Japan action center, at least partly, plays a role in the formation of the different vertical motion patterns over central-eastern China between the IO warm and cold summers. To do that, the quasigeostrophic omega equation is used to qualitatively diagnose the vertical motion. Ignoring diabatic heating and friction, the traditional omega equation indicates that the three-dimensional Laplacian operating on omega is forced by the vertical derivative of geostrophic vorticity advection and the horizontal Laplacian of the thermal advection (e.g., Holton 2004). However, the two forcing terms largely cancel each other, and it is difficult to isolate the primary physical process that induces the vertical motion. Therefore, we use a simplified version of the omega equation (Trenberth 1978; Holton 2004),

$$\left(\nabla^2 + \frac{f^2}{\sigma}\frac{\partial^2}{\partial p^2}\right)\omega \approx \frac{f}{\sigma}\left[\frac{\partial \mathbf{V}_g}{\partial p}\cdot\nabla(\zeta_g + f)\right], \qquad (1)$$

where ω denotes the vertical motion in isobaric coordinates, $\mathbf{V}_g$ stands for the horizontal geostrophic wind velocity, ζ_g stands for geostrophic vorticity, f stands for Coriolis parameter, and σ stands for static stability. The meanings of the other symbols are standard. Since we perform only a qualitative diagnosis, we substitute the relative vorticity and rotational thermal wind for the geostrophic relative vorticity and geostrophic thermal wind to simplify our calculation.

It should be noted that geostrophic approximation might not be applicable to the tropical regions; however, the diagnostic results from quasigeostrophic omega equation are still meaningful since we focus on the vertical motions over central-eastern China (poleward of about 30°N). We should also notice that although the term on the rhs is viewed as a forcing since the ω field is intimately associated with it, but it is not in the sense of causality. The physical essence of the omega equation only describes a consistence between the vorticity advection by the thermal wind and the vertical motion: that is, positive (negative) geostrophic vorticity advections by the geostrophic thermal wind correspond to ascending (descending) motions. This is because positive (negative) vorticity advections denote decreasing (increasing) thickness in that region. To maintain the hydrostatic constrain, without a diabatic heating, the vertical motion must be ascending (descending) to produce adiabatic cooling (heating). Therefore, the anomalous vorticity advection can "force" anomalous vertical motion.

Figure 5 shows the 1000–100-hPa averaged results of anomalous rotational thermal wind zonal advection [T_ZA = $(\partial u_\psi/\partial p)(\partial\zeta/\partial x)$] and meridional advection {T_MA = $(\partial v_\psi/\partial p)[\partial(\zeta + f)/\partial y]$} regressed against the daily tropical WNP convection index for the IO warm and cold summers and their differences (IO cold summers minus IO warm summers). It is noted that the T_MA term induces negative anomalous vorticity advection (corresponding to the anomalous descending motion) over the tropical WNP and positive anomalous vorticity advection (corresponding to the anomalous ascending motion) over subtropical East Asia, especially in the IO warm summers (see Fig. 5b). This means that, even under the dry dynamic framework (ignoring diabatic heating), the reverse anomalous vertical motions between the tropical WNP and subtropical East Asia tend to be induced by the meridional advection of the anomalous relative vorticity, which is consistent with Kosaka and Nakamura (2010, see their section 5b).

In the difference of the total vorticity advection (T_ZA + T_MA) between the IO warm and cold summers (see Fig. 5j), at the extratropical regions, the positive (negative) anomalous vorticity advection is well collocated with anomalous ascending (descending) motion shown in Fig. 3c. This indicates that our omega equation diagnosis's results are reasonable. There are very pronounced differences between the results of the T_ZA term in the IO warm and cold summers (see Figs. 5a,d). In the IO warm (cold) summers, there is a positive (negative) vorticity advection around the adjacent regions of Yellow

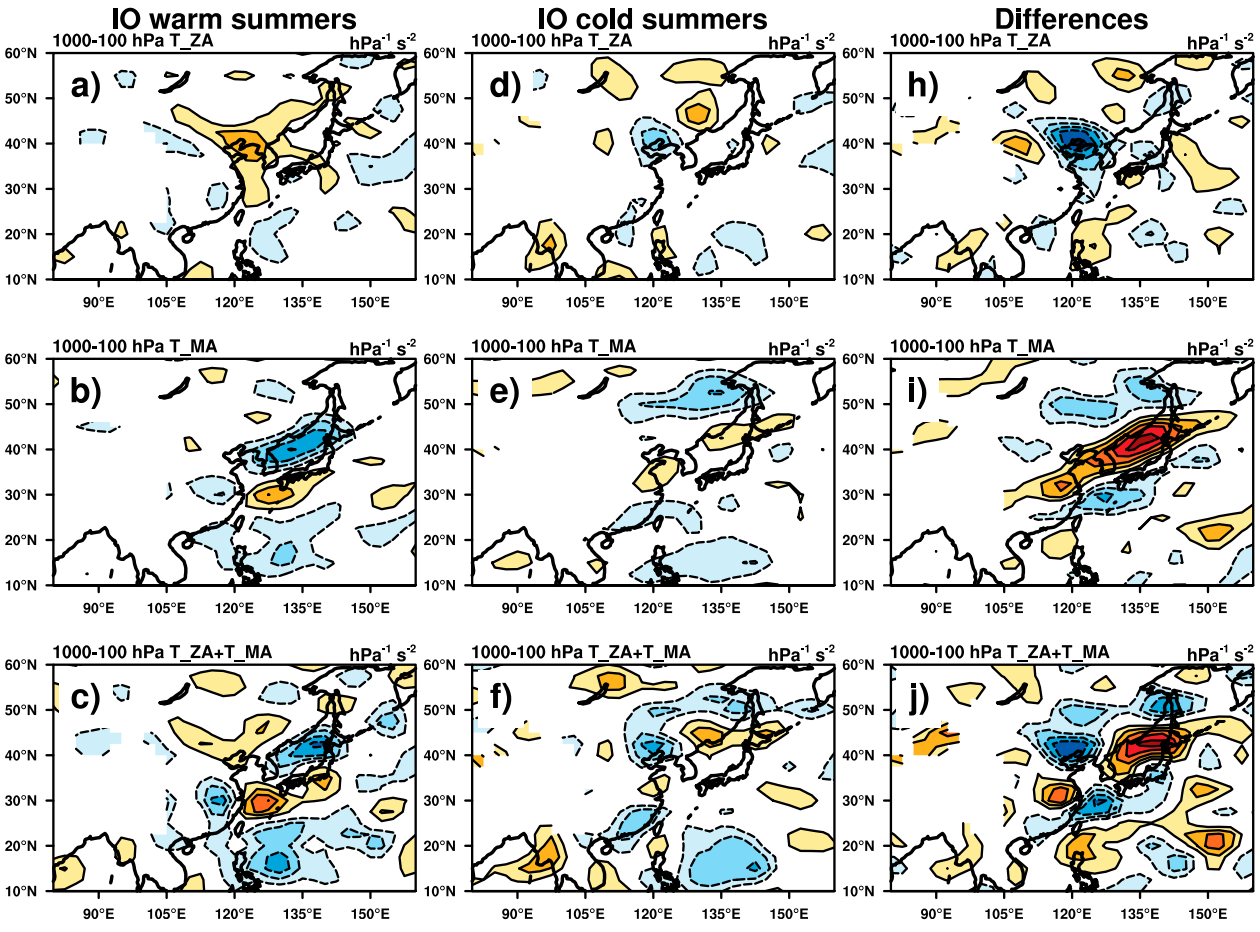

FIG. 5. As in Fig. 1, but for the 1000–100-hPa averaged results of anomalous T_ZA terms, T_MA terms, and T_ZA plus T_MA terms in the ω equation. (a)–(c) The IO warm summers, (d)–(f) the IO cold summers, and (h)–(j) their differences. Solid (dashed) contours represent positive (negative) values and the zero contours are omitted. The contour interval is 8×10^{-15} hPa^{-1} s^{-2}. To get a better visual effect, the positive (negative) values are shaded by the warm (cool) tone.

Sea and the Bohai Sea. Therefore, relative to the IO warm summers, there is an negative vorticity advection around the adjacent regions of Yellow Sea and the Bohai Sea in the IO cold summers (see Fig. 5h), which not only induces the anomalous descending motion over there but also counteracts the positive vorticity advection by the T_MA term over the north part of central-eastern China (see Fig. 5i) and thus results in weak anomalous ascending motion over that region as we observed in Fig. 3b.

It is noted that the anomalous T_ZA $[(\partial u_\psi/\partial p)(\partial\zeta/\partial x)]'$ associated with the WNP convection is dominated by the zonal advection of the anomalous geostrophic relative vorticity associated with the WNP convection by the background rotational thermal zonal wind $(\partial\overline{u_\psi}/\partial p)(\partial\zeta'/\partial x)$. The overbar and prime denote time mean and the anomalies associated with the WNP convection, respectively. We find that the northwestward displacement of the Japan action center leads to positive zonal gradients of the anomalous vorticity $\partial\zeta'/\partial x$ over the Yellow Sea and the Bohai Sea in the IO cold summers, which collocate well with the negative vorticity advection of the T_ZA term over there (not shown). These results indicate that, under the summer monsoon background flow in East Asia, the differences of the T_ZA term between the IO warm and cold summers are caused primarily by differences in the zonal gradient of the anomalous vorticity, which is obviously related to the northwestward displacement of the Japan action center. Therefore, we argue that the northwestward shift of the Japan action center of the PJ pattern plays a role in the formation of the different vertical motion patterns between the IO warm and cold summers as well.

5. Discussion about the northwestward displacement of the Japan action center

Since we argue that the northwestward displacement of the Japan action center plays a key role in the formation

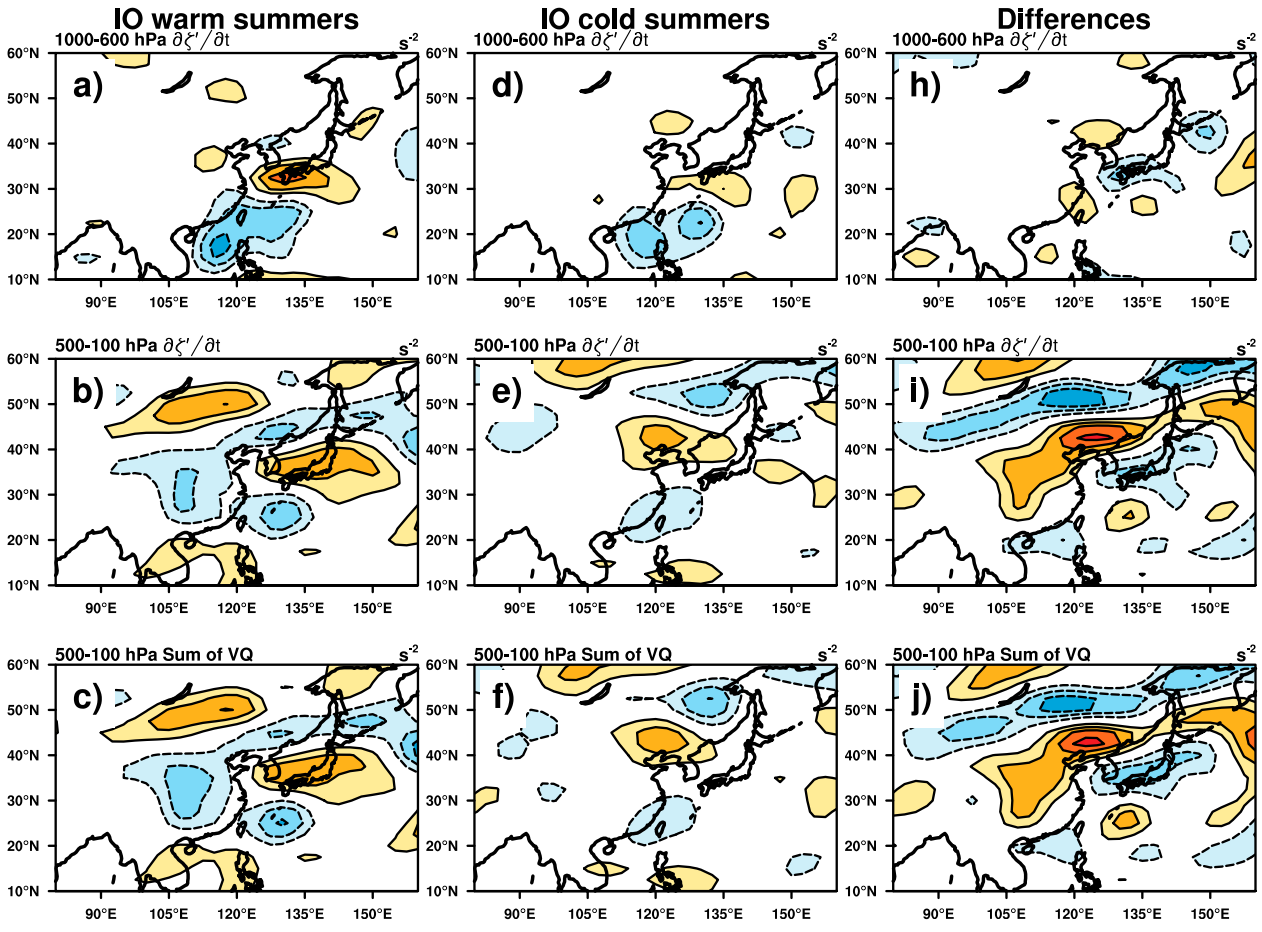

FIG. 6. Averaged lower-troposphere (mean result of 1000–600 hPa) and upper-troposphere (mean result of 500–100 hPa) tendency of the anomalies vorticity and sum of nine terms of the VQ plus the residual term associated with the WNP convection activities from lag −6 to −1 day during the IO warm and cold summers and their differences. (a)–(c) The IO warm summers, (d)–(f) the IO cold summers and (h)–(j) their differences (IO cold summers minus IO warm summers). Solid (dashed) contours represent positive (negative) values and the zero contours are omitted. The contour interval is $4 \times 10^{-12}\,s^{-2}$. To get a better visual effect, the positive (negative) values are shaded by the warm (cool) tone.

of different precipitation patterns in the IO warm and cold summers (thus the contrasting seesaw relationship), we discuss its plausible reason in this section.

First, the time evolution of vorticity anomalies associated with the WNP convection activities at 1000–100-hPa levels are acquired by using lead–lag regression (from lag −6 to −1 day). Then the tendencies of the anomalous vorticity ($\partial\zeta'/\partial t$) are calculated based on the lead–lag regressed vorticity anomalies. Figure 6 shows the averaged tendency of the anomalies vorticity associated with the WNP convection activities from lag −6 to −1 day for the lower troposphere (mean result of 1000–600 hPa) and upper troposphere (mean result of 500–100 hPa) during the IO warm and cold summers and their differences (IO cold summers minus IO warm summers). From WNP to south Japan, patterns of the tendency of the anomalous vorticity for either the lower and upper troposphere are a meridional dipole denoting the growth of the PJ pattern. However, compared to the IO warm summers overall, there is a positive vorticity tendency over the west of Japan during the IO cold summers (see Fig. 6e), which drives/maintains the northwestward displacement of the Japan action center during the IO cold summers.

In the differences of the vorticity tendency between the IO warm and cold summers for the upper troposphere (see Fig. 6i), there is a triple pattern characterized by a negative–positive–negative distribution (from north to south), consistent with the differences of the anomalous vorticity shown in Fig. 4h. This result indicates that the northwestward displacement of the Japan action center is well depicted in our calculation about the anomalous vorticity tendency. However, such a feature is not clear in the lower troposphere (see Fig. 6h),

suggesting that the northwestward displacement of the Japan action center is primarily occurred in the upper troposphere, which is consistent with the results shown in Fig. 4.

To understand what physical processes induce the northwestward displacement of the Japan action center, we calculate the vorticity tendency budget by using the vertical vorticity equation (VQ) in isobaric coordinates. According to the momentum equations in isobaric coordinates, the frictionless potential vorticity equation can be written as

$$\frac{D}{Dt}\left[\frac{-\partial v}{\partial p}\frac{\partial \theta}{\partial x}+\frac{\partial u}{\partial p}\frac{\partial \theta}{\partial y}+(\zeta+f)\frac{\partial \theta}{\partial p}\right] = \frac{-\partial v}{\partial p}\frac{\partial}{\partial x}\left(\frac{D\theta}{Dt}\right)+\frac{\partial u}{\partial p}\frac{\partial}{\partial y}\left(\frac{D\theta}{Dt}\right)+(\zeta+f)\frac{\partial}{\partial p}\left(\frac{D\theta}{Dt}\right). \tag{2}$$

Therefore, the vertical vorticity equation including the explicit contribution of thermodynamic elements in isobaric coordinates is

$$\frac{\partial \zeta}{\partial t}=-u\frac{\partial \zeta}{\partial x}-v\frac{\partial(\zeta+f)}{\partial y}-\omega\frac{\partial \zeta}{\partial p}+\frac{1}{\partial\theta/\partial p}(\zeta+f)\frac{\partial Q}{\partial p}+\frac{1}{\partial\theta/\partial p}\frac{-\partial v}{\partial p}\frac{\partial Q}{\partial x}+\frac{1}{\partial\theta/\partial p}\frac{\partial u}{\partial p}\frac{\partial Q}{\partial y} -(\zeta+f)\frac{1}{\partial\theta/\partial p}\frac{D}{Dt}\left(\frac{\partial \theta}{\partial p}\right)-\frac{1}{\partial\theta/\partial p}\frac{D}{Dt}\left(\frac{-\partial v}{\partial p}\frac{\partial \theta}{\partial x}\right)-\frac{1}{\partial\theta/\partial p}\frac{D}{Dt}\left(\frac{\partial u}{\partial p}\frac{\partial \theta}{\partial y}\right). \tag{3}$$

The variable ζ is the vertical vorticity in isobaric coordinates. Here, $Q = D\theta/Dt$ denotes the diabatic heating, which is estimated as a residual of the thermodynamic equation using the scheme of Yanai et al. (1973). The meanings of the other symbols are standard. The first, second, and third terms of the rhs denote vorticity tendency associated with the zonal, meridional, and vertical advections of vorticity, referred to as the ZA, MA, and VA terms, respectively. The fourth, fifth, and sixth terms of the rhs represent the vorticity tendency due to diabatic heating, referred to as the DH_P, DH_X, and DH_Y terms, respectively. The seventh, eighth, and ninth terms of the rhs are the contributions of vorticity tendency associated with the slants of the isentropic levels, subsequently referred to as the Theta_P, Theta_X, and Theta_Y terms. Liu et al. (2013) and references therein provide more details about the vertical vorticity equation explicitly, including the thermodynamical contribution.[1]

Based on this equation, we calculate contributions of the all nine terms to the daily $\partial\zeta/\partial t$ (calculated based on the time evolution of the vorticity field) in the 26 summers that data cover. A residual term is also acquired by subtracting the sum of the all nine terms from $\partial\zeta/\partial t$. The residual term denotes the physical processes that our VQ does not include such as friction and viscous dissipations. Similar to the analysis of the time evolution of vorticity anomalies associated with the WNP convection activities, the calculations of the lead–lag regression are applied on the anomalous ZA to residual terms. Figures 6c,f,j show the sum of regressed nine terms of the VQ plus the residual term averaging from lag −6 to −1 day for the upper troposphere during the IO warm and cold summers and their differences (IO cold summers minus IO warm summers). The patterns of the sum of the all terms in the VQ are well match with the patterns of $\partial\zeta'/\partial t$ shown in Figs. 6b,e,i, indicating that our vorticity budget diagnoses are precise.

From the results of the VQ, we find that, in the upper troposphere, the MA term produces positive vorticity tendency around the west of Japan but is greatly compensated by the ZA term. Other terms are smaller by an order of magnitude than the ZA and MA terms over the adjacent regions of Japan in either the IO warm and cold summers (not shown). Based on these results, we might argue that the variability in the Japan action center is determined primarily by the ZA and MA terms. If we assume that contributions of the nonlinear terms are small,[2] then the MA anomalies associated with the WNP convection can be decomposed as

$$\mathrm{MA}' \approx -\overline{v}\partial\zeta'/\partial y - v'\partial(\overline{\zeta}+f)/\partial y.$$

Here, bars and primes denote time mean and the anomalies associated with the WNP convection. Because $\partial(\overline{\zeta}+f)/\partial y$ is strong and v' is comparable to $\overline{v}$, MA′ is usually dominated by $-v'\partial(\overline{\zeta}+f)/\partial y$. Therefore, high value regions of the vorticity tendency produced by the

[1] It must be noted that the vertical vorticity equation in Liu et al. (2013) is in Cartesian coordinates. It contains the divergence term, which is implicit in the vorticity equation of isobaric coordinates.

[2] This assumption is reasonable when the anomalous vorticity is weak.

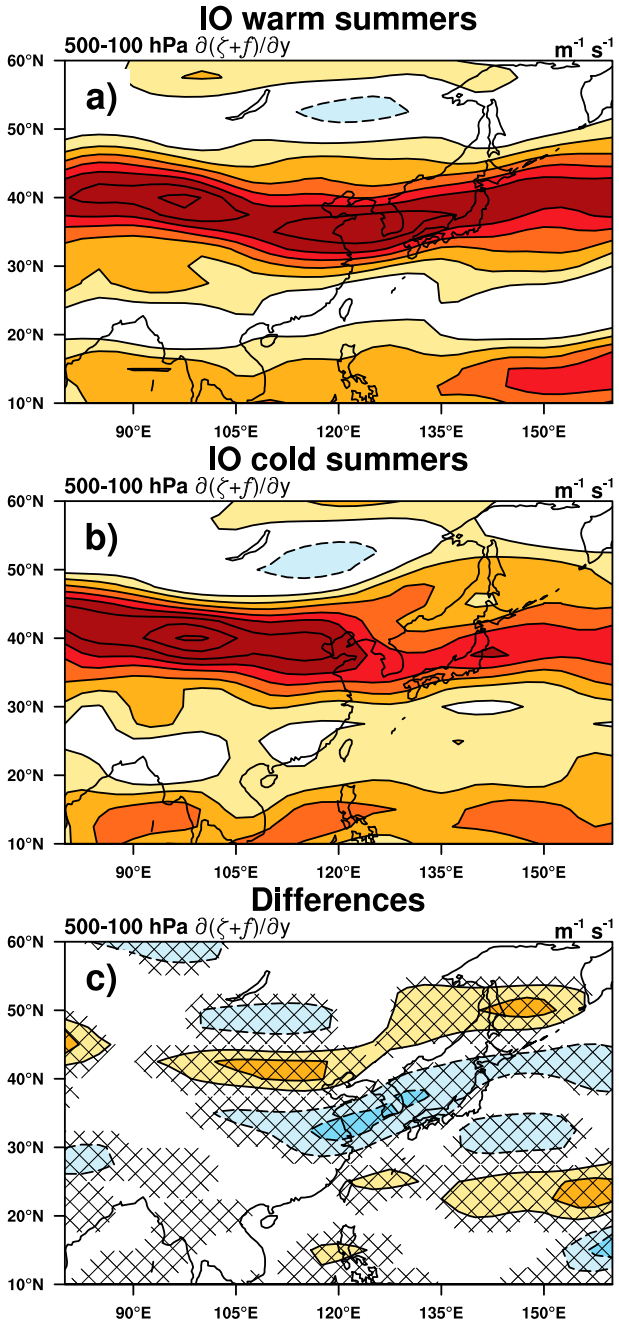

FIG. 7. Summer mean meridional gradients of absolute vorticity averaged from 500 to 100 hPa for (a) the IO warm summers and (b) the IO cold summers and (c) their differences (IO cold summers minus IO warm summers). The differences at the 95% confidence level are hatched. Solid (dashed) contours represent positive (negative) values and the zero contours are omitted. The contour interval is $1 \times 10^{-11}\,\mathrm{m^{-1}\,s^{-1}}$. To get a better visual effect, the positive (negative) values are shaded by the warm (cool) tone.

MA term would tend to follow the high value regions of $\partial(\overline{\zeta}+f)/\partial y$.

To support this argument, Fig. 7 shows the summer mean $\partial(\overline{\zeta}+f)/\partial y$ averaging from 1000 to 500 hPa for the IO warm and cold summers and their differences (IO cold summers minus IO warm summers). Xie et al. (2009) argued that the warming (cooling) of the IO increases (decreases) the tropospheric temperature, triggering a baroclinic Kelvin wave into the Pacific. In the WNP, the Kelvin wave might induce an anomalous divergence (convergence) because of the surface friction, which suppresses (enhances) the convection triggering/maintaining the anomalous anticyclone (cyclone) over there. Therefore, as shown in Fig. 7, $\partial(\overline{\zeta}+f)/\partial y$ over subtropical to midlatitude East Asia (30°–45°N, 110°–140°E) is stronger (weaker) in the IO warm (cold) summers. Thus, $\partial(\overline{\zeta}+f)/\partial y$ over subtropical to midlatitude East Asia in the IO cold summers has a northwestward shifting compared to the IO warm summer (see Fig. 7c).

We find that the positive vorticity tendency over the adjacent regions of Japan in the upper troposphere shown in Fig. 6 is roughly collocated with the high value regions of $\partial(\overline{\zeta}+f)/\partial y$ in either the IO warm and cold summers (see Figs. 6b,e). More important is that the pattern of the differences in $\partial(\overline{\zeta}+f)/\partial y$ between the IO warm and cold summers (see Fig. 7c) roughly matches with the differences in vorticity tendency shown in Fig. 6i. Therefore, we might argue that, because of the northwestward shifting of $\partial(\overline{\zeta}+f)/\partial y$ in the IO cold summers, the positive vorticity tendency produced by the MA term also tends to displace northwestward since high value regions of the vorticity tendency produced by the MA term would tend to follow the high value regions of $\partial(\overline{\zeta}+f)/\partial y$, which induces the northwestward displacement of the Japan action center in the IO cold summers.

We should underscore that the ZA and MA terms have opposite signs and offset from each other greatly. The actual $\partial\zeta'/\partial t$ is a residual sum resulting from a competition among ZA, MA, and the other seven terms in the VQ and the residual term. Magnitudes of other terms are much smaller than that of the ZA and MA terms over the adjacent regions of Japan; however, many of them are comparable to the actual $\partial\zeta'/\partial t$. Therefore, the foregoing argument about the northwestward displacement of the Japan action center is only a possible explanation. We should also point out that structures and magnitudes of the tropical convection anomalies regressed onto the daily WNP convection index between the IO warm and cold summers have no apparent differences (not shown). This precludes a possibility that the northwestward displacement of the

Japan action center in the IO cold summers is a result of the different structures or magnitudes in the tropical convection anomalies.

6. Summary and discussion

a. Summary

The seesaw relationship between tropical western North Pacific (WNP) convection activities and anomalous precipitation over subtropical East Asia is important for understanding and predicting the variability of the East Asia summer monsoon (EASM) since it reflects the dominant variability of the EASM. In this study, we use daily data to examine and compare the subseasonal seesaw relationship when the summer mean Indian Ocean (IO) SST is both warmer and colder than normal. Our analyses show the following:

1) The precipitation anomalies over central-eastern China associated with the anomalous convection activities of the tropical WNP during the IO cold summers are much weaker and less evident compared to those in the IO warm summers.
2) There are greater anomalous moisture fluxes converging over central-eastern China during the IO warm summers. In contrast, the converging regions of the anomalous moisture flux shrink obviously during the IO cold summers.
3) In contrast to the evident anomalous ascending motion during the IO warm summers, the anomalous ascending motion over central-eastern China during the IO cold summers becomes weaker.

All these findings indicate there is a contrast in the seesaw relationship between the IO warm and cold summers. The subseasonal seesaw relationship in the IO cold summers becomes obscure. The distinct seesaw relationship between the IO warm and cold summers can be directly attributed to the very different anomalous moisture transportations and vertical motions over central-eastern China.

To understand the contrast in the seesaw relationship, particularly for the weakening seesaw relationship during the IO cold summers, we examine the Pacific–Japan (PJ) patterns associated with the anomalous tropical WNP convection in terms of vorticity anomalies. Regressed vorticity anomalies show that the positions of the Japan action center of the PJ pattern during the IO warm and cold summers are different. Compared to the IO warm summers, the Japan action center has an evident northwestward displacement in the IO cold summers. We argue that the northwestward shift of the Japan action center plays a key role in determining the weakening seesaw relationship during the IO cold summers. The primary physical processes are summarized as follows: During the IO cold summers, the time mean meridional gradient of absolute vorticity ($\partial(\overline{\zeta}+f)/\partial y$) over subtropical to midlatitude East Asia has a northwestward displacement. Vertical vorticity tendency budget diagnoses show that the vorticity tendency over the adjacent regions of Japan is determined primarily by the ZA and MA terms. Since the MA term is dominated by $-v'\partial(\overline{\zeta}+f)/\partial y$, high value regions of the vorticity tendency produced by the MA term would tend to follow the high value regions of $\partial(\overline{\zeta}+f)/\partial y$. Thus, the northwestward shifting $\partial(\overline{\zeta}+f)/\partial y$ leads to the positive vorticity tendency produced by the MA term also tends to displace northwestward, which possibly induces the northwestward displacement of the Japan action center in the IO cold summers. Because of the northwestward displacement of the Japan action center, there are anomalous northerlies over the north part of central-eastern China resist the anomalous northeastward moisture transportation. Besides that, the omega equation shows that, under the summer monsoon background flow in East Asia, the northwestward shifting of the Japan action center induces anomalous negative vorticity advections by the thermal wind around the adjacent regions of Yellow Sea and the Bohai Sea. Without a diabatic heating, the vertical motion must be descending to produce adiabatic heating to maintain the hydrostatic constrain. Therefore, the anomalous moisture transportation and vertical motion suppress positive precipitation anomalies over the north part of central-eastern China, resulting in a remarkable weakening of the seesaw relationship during the IO cold summers.

b. Discussion

Kosaka and Nakamura (2010) showed that the anomalous vertical motions, induced by dry physical processes only, correspond well with the anomalous precipitation associated with the PJ pattern but is substantially weaker than the observational results. This suggests that the dynamically forced anomalous vertical motion associated with the PJ pattern tends to trigger or reinforce the anomalous precipitation accompanying this pattern. Meanwhile, the diabatic heating associated with the anomalous precipitation also plays a role in refueling the observed anomalous vertical motion. Figure 8 shows daily diabatic heating Q anomalies at 400 hPa regressed against the tropical WNP convection daily index during the IO warm and cold summers. It is clear that the intensity and domain of the anomalous diabatic heating over the central-eastern China are greater in the IO warm summers. Therefore, the diabatic heating associated with anomalous precipitation also plays a role in

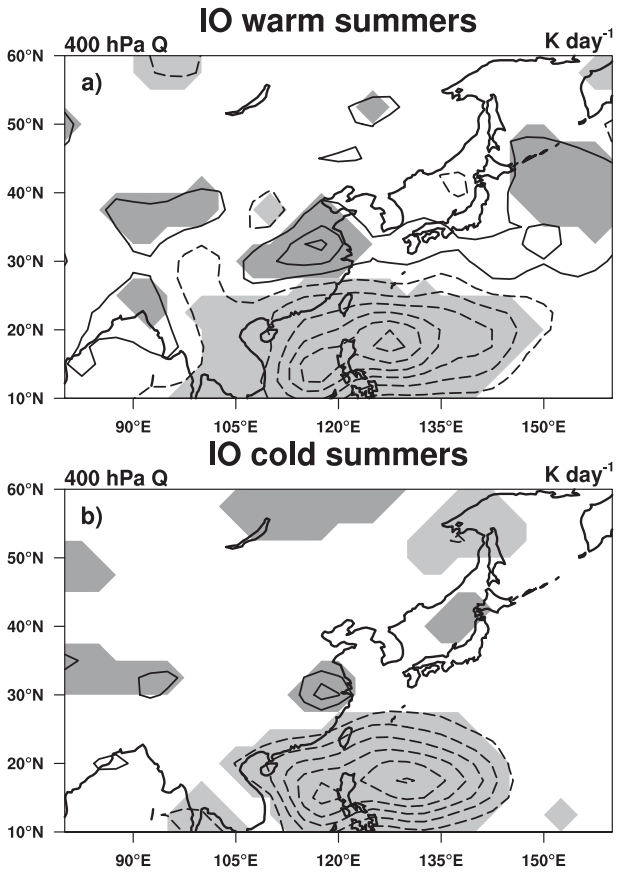

FIG. 8. Anomalous daily Q at 400 hPa regressed onto the daily tropical WNP convection index during the IO (a) warm and (b) cold summers. Solid (dashed) contours represent positive (negative) values and the zero contours are omitted. The regressed results at the 95% confidence level are shaded. The contour interval is 0.5 K day^{-1}.

the formation of the different anomalous vertical motion between the IO warm and cold summers and thus the contrasting seesaw relationship. Besides that, no evident diabatic cooling is found over the adjacent regions of Yellow Sea and the Bohai Sea, where the vertical motion is descending in the IO cold summers. This result supports our omega equation diagnosis that the descending motion around these regions is dynamically induced.

In addition to the tropical north–south orientation PJ teleconnection pattern, the fluctuations of the precipitation over central-eastern China are also closely related to an extratropical west–east orientation wavelike teleconnection pattern: the Silk Road (SR) pattern (e.g., Enomoto et al. 2003; Yasui and Watanabe 2010; and references therein). Hsu and Lin (2007) defined a tripole rainfall pattern to delineate the dominant interannual variability of precipitation of East Asian summer. The positive (negative) phase of the tripole pattern denotes there is more (less) rainfall in central-eastern China, Japan, and South Korea. An intriguing phenomenon is reported by Hsu and Lin (2007) that the PJ (SR) pattern is more evident in the positive (negative) phase of the tripole pattern. The reasons responsible for this phenomenon are still unclear. Hsu and Lin (2007) also found that the jet over subtropical to midlatitude of East Asia shifts northward in the negative phase of the tripole pattern [see Fig. 11 of Hsu and Lin (2007)]. We notice that the jet over subtropical to midlatitude of East Asia has a very similar northward displacement in the IO cold summers (not shown). Therefore, we infer that tropical connection (the PJ pattern) is not clear in the negative phase of the tripole pattern and is similar to the scenario in the IO cold summers that a northwestward-shifting Japan action center resulting from variations of background flow tends to suppress the influences of the PJ pattern on the variability of the precipitation over central-eastern China.

Some previous studies have noted that the wave train triggered by tropical WNP convection activities and rainfall might cross the North Pacific and extend to North America in the upper troposphere (e.g., Nitta 1987; Wang and Lau 2001; Lin 2009; Ding et al. 2011). Interestingly, we find that the wave trains associated with tropical WNP convection in the upper troposphere during the IO warm and cold summers are also different. Figure 9 shows the regressed daily meridional wind anomalies at the 200-hPa level against the daily WNP convection index during the IO warm and cold summers. The tropical WNP convection activities are associated with a downstream-propagating wave train similar to a circumglobal teleconnection pattern during the IO warm summers, suggesting that the influences of tropical WNP convection are global. However, the responses in the upper troposphere during the IO cold summers are rather local. Therefore, the influences of tropical WNP convection are confined to East Asia.

The physical mechanisms responsible for the different upper-troposphere circulation responses are still unclear. We hypothesize that this difference might be related to the following: 1) The very different anomalous precipitation, diabatic heating, or vertical motion associated with the tropical WNP convection over central-eastern China during the IO warm and cold summers: The stronger (weaker) anomalous precipitation, diabatic heating, or vertical motion over central-eastern China in the IO warm (cold) summers might lead to a stronger (weaker) response along the Eurasian jet in the upper troposphere. 2) The different background flow in the upper troposphere during the IO warm and cold summers: Tsuyuki and Kurihara (1989) noted that the anomalous tropical WNP convection is accompanied by

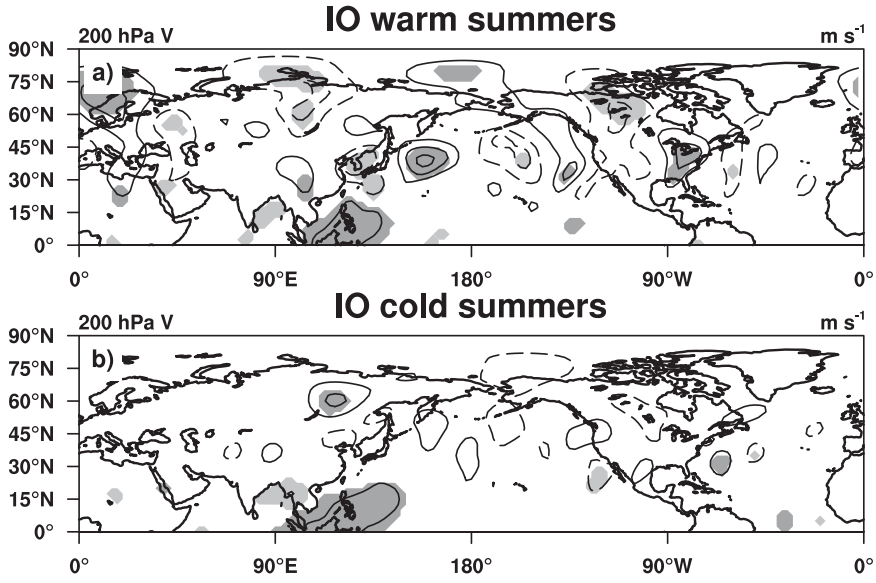

FIG. 9. As in Fig. 8, but for anomalous daily meridional wind at 200 hPa. The contour interval is 1 m s^{-1}.

a wave train that originates in the tropical WNP, crosses the North Pacific, and extends to the west coast of North America during midsummer (from mid-July to early September), while this wave train is hardly observed during the rainy season in East Asia (from early June to mid-July). They argued that this difference could be attributed to the different barotropic unstable modes (Simmons et al. 1983) as a result of the different background circulation. The different wave trains triggered by tropical WNP convection activities in the midlatitudes during the IO warm and cold summers deserve a further investigation but are beyond the scope of this study.

Acknowledgments. The authors appreciate the helpful comments by three anonymous reviewers. This study is sponsored by the 973 program (Grant 2010CB950401) and National Nature Science Foundation of China (Grant U0833602). JS is also supported by the National Nature Science Foundation of China (Grant 41275086).

REFERENCES

Bretherton, C. S., M. Widmann, V. P. Dymnikov, J. M. Wallace, and I. Bladé, 1999: The effective number of spatial degrees of freedom of a time-varying field. *J. Climate,* **12,** 1990–2009, doi:10.1175/1520-0442(1999)012<1990:TENOSD>2.0.CO;2.

Ding, Q. H., B. Wang, J. M. Wallace, and G. Branstator, 2011: Tropical–extratropical teleconnections in boreal summer: Observed interannual variability. *J. Climate,* **24,** 1878–1896, doi:10.1175/2011JCLI3621.1.

Enomoto, T., B. J. Hoskins, and Y. Matsuda, 2003: The formation mechanism of the Bonin high in August. *Quart. J. Roy. Meteor. Soc.,* **129,** 157–178, doi:10.1256/qj.01.211.

Holton, J. R., 2004: *An Introduction to Dynamic Meteorology.* 4th ed. Elsevier Academic Press, 535 pp.

Hsu, H. H., and S. M. Lin, 2007: Asymmetry of the tripole rainfall pattern during the East Asian summer. *J. Climate,* **20,** 4443–4458, doi:10.1175/JCLI4246.1.

Huang, G., 2004: An index measuring the interannual variation of the East Asian summer monsoon—The EAP index. *Adv. Atmos. Sci.,* **21,** 41–52, doi:10.1007/BF02915679.

Huang, R. H., and F. Y. Sun, 1992: Impacts of the tropical western Pacific on the East Asia summer monsoon. *J. Meteor. Soc. Japan,* **70,** 243–256.

Kalnay, E., and Coauthors, 1996: The NCEP/NCAR 40-Year Reanalysis Project. *Bull. Amer. Meteor. Soc.,* **77,** 437–471, doi:10.1175/1520-0477(1996)077<0437:TNYRP>2.0.CO;2.

Kosaka, Y., and H. Nakamura, 2006: Structure and dynamics of the summertime Pacific-Japan teleconnection pattern. *Quart. J. Roy. Meteor. Soc.,* **132,** 2009–2030, doi:10.1256/qj.05.204.

——, and ——, 2010: Mechanisms of meridional teleconnection observed between a summer monsoon system and a subtropical anticyclone. Part I: The Pacific–Japan pattern. *J. Climate,* **23,** 5085–5108, doi:10.1175/2010JCLI3413.1.

Kurihara, K., and T. Tsuyuki, 1987: Development of the barotropic high around Japan and its association with Rossby wave-like propagation over the North Pacific: Analysis of August 1984. *J. Meteor. Soc. Japan,* **65,** 237–246.

Kwon, M. H., J.-G. Jhun, B. Wang, S.-I. An, and J.-S. Kug, 2005: Decadal change in relationship between East Asian and WNP summer monsoons. *Geophys. Res. Lett.,* **32,** L16709, doi:10.1029/2005GL023026.

Lee, E. J., J. G. Jhun, and C. K. Park, 2005: Remote connection of the northeast Asian summer rainfall variation revealed by a newly defined monsoon index. *J. Climate,* **18,** 4381–4393, doi:10.1175/JCLI3545.1.

Li, J. P., and Q. C. Zeng, 2002: A unified monsoon index. *Geophys. Res. Lett.,* **29,** doi:10.1029/2001GL013874.

Lin, H., 2009: Global extratropical response to diabatic heating variability of the Asian summer monsoon. *J. Atmos. Sci.,* **66,** 2697–2713, doi:10.1175/2009JAS3008.1.

Lin, Z., R. Lu, and W. Zhou, 2009: Change in early-summer meridional teleconnection over the western North Pacific and

East Asia around the late 1970s. *Int. J. Climatol.*, **30,** 2195–2204, doi:10.1002/joc.2038.

Liu, B., G. Wu, J. Mao, and J. He, 2013: Genesis of the South Asian high and its impact on the Asian summer monsoon onset. *J. Climate,* **26,** 2976–2991, doi:10.1175/JCLI-D-12-00286.1.

Lu, R. Y., 2001: Interannual variability of the summertime North Pacific subtropical high and its relation to atmospheric convection over the warm pool. *J. Meteor. Soc. Japan,* **79,** 771–783, doi:10.2151/jmsj.79.771.

——, and Z. D. Lin, 2009: Role of subtropical precipitation anomalies in maintaining the summertime meridional teleconnection over the western North Pacific and East Asia. *J. Climate,* **22,** 2058–2072, doi:10.1175/2008JCLI2444.1.

Nitta, T., 1987: Convective activities in the tropical western Pacific and their impact on the Northern Hemisphere summer circulation. *J. Meteor. Soc. Japan,* **74,** 425–445.

Simmons, A. J., J. M. Wallace, and G. W. Branstator, 1983: Barotropic wave propagation and instability, and atmospheric teleconnection patterns. *J. Atmos. Sci.,* **40,** 1363–1392, doi:10.1175/1520-0469(1983)040<1363:BWPAIA>2.0.CO;2.

Trenberth, K. E., 1978: On the interpretation of the diagnostic quasi-geostrophic omega equation. *Mon. Wea. Rev.,* **106,** 131–137, doi:10.1175/1520-0493(1978)106<0131:OTIOTD>2.0.CO;2.

——, G. W. Branstator, D. Karoly, A. Kumar, N.-C. Lau, and C. Ropelewski, 1998: Progress during TOGA in understanding and modeling global teleconnections associated with tropical sea surface temperatures. *J. Geophys. Res.,* **103,** 14 291–14 324, doi:10.1029/97JC01444.

Tsuyuki, T., and K. Kurihara, 1989: Impact of convective activity in the western tropical Pacific on the East Asian summer circulation. *J. Meteor. Soc. Japan,* **67,** 231–247.

Wang, B., and K. M. Lau, 2001: Interannual variability of the Asian summer monsoon: Contrasts between the Indian and the western North Pacific–East Asian monsoons. *J. Climate,* **14,** 4073–4090, doi:10.1175/1520-0442(2001)014<4073:IVOTAS>2.0.CO;2.

——, Z. Wu, J. Li, J. Liu, C.-P. Chang, Y. Ding, and G. Wu, 2008: How to measure the strength of the East Asian summer monsoon. *J. Climate,* **21,** 4449–4463, doi:10.1175/2008JCLI2183.1.

Wu, B., T. J. Zhou, and T. Li, 2009: Seasonally evolving dominant interannual variability modes of East Asian climate. *J. Climate,* **22,** 2992–3005, doi:10.1175/2008JCLI2710.1.

Wu, R. G., and B. Wang, 2002: A contrast of the East Asian summer monsoon–ENSO relationship between 1962–77 and 1978–93. *J. Climate,* **15,** 3266–3279, doi:10.1175/1520-0442(2002)015<3266:ACOTEA>2.0.CO;2.

Xie, S. P., K. Hu, J. Hafner, H. Tokinaga, Y. Du, G. Huang, and T. Sampe, 2009: Indian Ocean capacitor effect on Indo–western Pacific climate during the summer following El Niño. *J. Climate,* **22,** 730–747, doi:10.1175/2008JCLI2544.1.

Yanai, M., S. Esbensen, and J.-H. Chu, 1973: Determination of bulk properties of tropical cloud clusters from large-scale heat and moisture budgets. *J. Atmos. Sci.,* **30,** 611–627, doi:10.1175/1520-0469(1973)030<0611:DOBPOT>2.0.CO;2.

Yasui, S., and M. Watanabe, 2010: Forcing processes of the summertime circumglobal teleconnection pattern in a dry AGCM. *J. Climate,* **23,** 2093–2114, doi:10.1175/2009JCLI3323.1.

Yatagai, A., K. Kamiguchi, O. Arakawa, A. Hamada, N. Yasutomi, and A. Kitoh, 2012: APHRODITE: Constructing a long-term daily gridded precipitation dataset for Asia based on a dense network of rain gauges. *Bull. Amer. Meteor. Soc.,* **93,** 1401–1415, doi:10.1175/BAMS-D-11-00122.1.

Yim, S.-Y., S.-W. Yeh, R. Wu, and J.-G. Jhun, 2008: The influence of ENSO on decadal variations in the relationship between the East Asian and western North Pacific summer monsoons. *J. Climate,* **21,** 3165–3179, doi:10.1175/2007JCLI1948.1.